Effect of additional Multi-Walled Carbon Nanotubes on characteristic of Ti-24Nb-4Zr-8Sn alloy

a)Hussein Khalil Burhan b)Jassim M. Salman and c) Nawal Mohammed Dawood
C0llege of Materials Engineering /Metallurgical Engineering Department, University of Babylon, Iraq
a) hm1.hm52@gmail.com
b) mat.jassim.mohammed@uobabylon.edu.iq
c) mat.newal.mohammed@uobabylon.edu.iq

Abstract

Due to its higher specific strength, superior corrosion resistance, and low density, titanium (Ti) and its alloys have found widespread application in petrochemical, aerospace, biomedical, and several other manufacturing. Throughout the years, Because of their exceptional qualities, carbon nanotubes have received attention in engineering materials research due to their outstanding and excellent properties. Owing to the demands for lightweight materials with extraordinary mechanical and thermal properties for diverse. The purpose of this study is to evaluate the effects of various percentages of multiwall carbon nanotubes(MWCNT) (0.1%, 0.2%, 0.3%, 0.4%) addition to Ti-24Nb-4Zr-8Sn(Ti2448) on phase compositions and macrostructures also mechanical properties such as wear resistance and hardness of Ti-24Nb-4Zr-8Sn- MWCNT composites fabricated by the powder metallurgy. Experimental results demonstrate the hardness increases with increases percentage of MWCNT reaching 172 HB with when addition of 0.4%, while the grain size and wet wear rate decreased with increasing the content of MWCNT reaching 23.7μm and $7.034*10^{-5}$ $\frac{g}{cm}$ respectively.

Keywords: Powder metallurgy; Ti-24Nb-4Zr-8Sn alloy; wear rate; Biomedical material

Introduction

The primary objective of medical research nowadays is the creation of novel biomaterials with enhanced biological and mechanical capabilities. Since the 1960s, titanium alloys have been commonly utilized in orthopedics, such as in dental implants and artificial joints, and they are still essential metals for usage in medicine today [1]. Ti-based materials have been shown to have a number of advantages, such as low density, high mechanical strength, moderate elastic modulus, great corrosion resistance, and biocompatibility. But whenever these materials are brushed against other metals or against themselves, they always suffer extreme wear and tear [2]. The primary reasons for aseptic loosening in long-term orthopedic implants, such as hip and knee replacements, are wear and subsequent osteolysis (bone tissue loss). However, Ti alloy metal wear particles have the potential to harm humans by causing metalloids and tissue blacking [3]. Because of their high coefficient of friction, titanium and its alloys are used in situations where wear resistance is not important [4]. As a result, there has been little progress in the usage of titanium and its alloys in clinical medicine. One method to get around these defects is to mix different materials to get better qualities than only the pure forms of each material. The ability to integrate the various qualities of metal and ceramic into a single system is the clearest benefit of ceramic-metal composites [5].

One of the most promising materials is titanium metal matrix composites (Ti MMCs), which include versions with powdered reinforcing particles [6]. In particular, weight reduction and improved mechanical qualities can be obtained by nanostructured reinforcements. Because of their high modulus, exceptional strength, and nanostructures, novel nanostructured reinforcements such as nanodiamonds (NDs), graphene (Gr), and multiwalled carbon nanotubes (CNTs), all contribute to the advance of new materials with excellent mechanical properties[7-9]. The development Ti-24Nb-4Zr-8Sn is a titanium alloy with a high strength of over 850 MPa and an unprecedentedly low initial

Young's modulus of 42 GPa. It was created by vacuum arc melting and the hot forged at 1123 K. Hao and associates [10]

Selective laser melting (SLM) was employed by L.C. Zhang et al. [11] to create biomedical β alloy Ti–24Nb–4Zr–8Sn components, one of which was an acetabular cup sample. Additionally, a comparison is made between the mechanical properties of the unprocessed material and those of traditionally processed material.

Using MIM, Fırat et al.[12] successfully demonstrated Ti–24Nb–4Zr–8Sn alloy samples that show an ultimate tensile strength ranging from (655 to 720 MPa) and a plastic elongation that varies from 2% to 9% depending on sintering settings. The lowermost Young's modulus, 54 GPa, is around 50% less than that of Ti–6Al–4V and CP Ti.

This study aims to influence the addition of MWCNT in different ratios to the Ti2448 alloy manufactured in a method of powder metallurgy and study the effect of adding this element on the microstructural assessment and mechanical characteristics of sintered specimens.

2. Experimental

2.1 Raw materials

The materials powders' purity and average particle size utilized when preparing are described in Table 1 along with its tests.

Table 1: The average particle size and Purity of powders

Material(Powder)	% Purity	(Average particle size (μm)	Source
Ti	99.5	47	Qingdao Hesiway Industrial Co., Ltd. China
Nb	99.9	19	SICHUAN POROUS METAL TECHNOLOGY CO., LTD. China
Zr	99	24	XIAN FUNCTION MATERIAL GROUP CO., LTD. China
Sn	99.9	11	ALPHA CHEMIKA Inc. India
MWCNT	90	outer diameter 10-30 nm Length 10-30 μm	Cheap Tubes Inc. Grafton, USA

Powdered Ti-24Nb-4Zr-8Sn, also known as Ti2448, contains multi-walled carbon nanotubes with different percentages of 0.1, 0.2, 0.3, and 0.4 were utilized as raw materials to create biomedical composites. Table (2) provides information on the code and composition of alloys used in this project.

Table (2): lists the codes and compositions of alloys.

NO	Alloy Code	Chemical Composition (wt.) %
1	M	Ti-24Nb-4Zr-8Sn
2	A1	Ti-24Nb-4Zr-8Sn+0.1 MWCNT
3	A2	Ti-24Nb-4Zr-8Sn+0.2 MWCNT
4	A3	Ti-24Nb-4Zr-8Sn+0.3 MWCNT
5	A4	Ti-24Nb-4Zr-8Sn+0.4 MWCNT

Metallic powders must be properly homogenized prior to compaction and sintering in order to get optimal results. Blending is a process that involves the mixing of powders that have the same content but may have varying particle sizes using the device type: Bench-Top Planetary Automatic Ball Mill, MTI Corporation. Distinct particle sizes are often combined to minimize porosity, whereas mixing is described as the process of combining powders of two or more different materials[10]. A planetary automated ball mill was utilized for the wet mixing of powders, and different-sized stainless steel balls were used for five hours to ensure a uniform distribution of the powder particles. Acetone was added to the mixing medium to make it moist.

To carry out the compacting procedure, a stainless steel mold with a 12.5 mm diameter was used. An electric-hydraulic press was used to compress 4 grams of mixture under pressure using a single channel device (type: CT340-CT440, American) (800 MPa). To construct a disk spaceman with a diameter and thickness of 12.5 mm and 4.5 mm, the holding time was 4 minutes. Paraffin is used as a lubricant in the pressing process to minimize friction.

The sintering process was carried out in a tube furnace, which involved heating the material from room temperature to 1250 °C with a heating rate of 5°C per minute and a stay time of 7 h in an argon atmosphere to inhibit the specimen's oxidation. Afterward, slow cooling in the furnace with continuous argon circumstances to the room temperature. The figure below shows the sample before and after the sintering process.

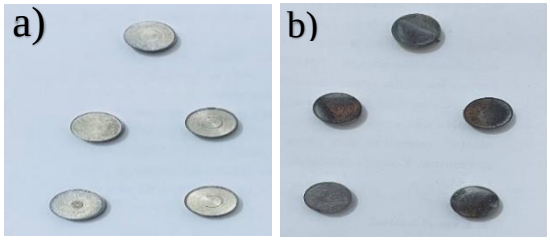

Figure (1): Sample a) before and b) after sintering

Substrates were made by using silicon carbide(SiC) emery sheets with grit sizes of 120, 220, 320,400, 600, 800,1000, 2000, and 3000 μm to grind the sample's surface. The substrate was then cleaned with distilled water. Next, the substrates were polished using a 1.5μm diamond paste utilizing a grinding and polishing machine to achieve a mirror-like smooth finish. According to ASTM [14], the etching was performed at room temperature using 2ml HF, 6ml HNO_3, and 92ml Distilled water[14],. The prepared for use samples were submerged in the etching solution for three to five seconds using the etching after which they were dried and cleaned with distilled water in order to prepare them for microstructure analysis.

2.2 Phase Identification

The test of X-ray diffraction analysis ((XRD 6000, Shimadzo, Japan) was taken so as to characterize the powder (Ti, Nb, Zr, Sn, and MWCNT) in the present work, also substrate alloy and reinforced samples, Cu Kα radiation (λ = 1.5405 Å) were used in the XRD, with a power of Kv/30 mA.

2.3 Microstructure test

The microscopic structure was studied using optical microscopy the microscope type (BEL PHOTONICS), in order to recognize the existing phases and to see the shape and size of the grains, after grinding, polishing, and etching in a solution.

Grain size and grain size distribution have significant effects on structure and mechanical properties. So, longitudinal-section for grain measured by 2D-image analysis approach based on scanning electron microscopy via analyzing and processing of incorporating digital image. used TESCAN 2D-visualization &analysis software16.

Scanning Electron Microscopy (SEM) inception is among the most extensively usage surface examination methods, allowing for the observation of a wide variety of scales and features. In the present work, SEM-type VEGA 3 SBU was used to reveal the microstructure of the matrix and reinforcement. It was used to characterize the morphology and microstructure of the sintered samples.

The analytical technique that was used for chemical analysis and elemental analysis of the implant's surface after sintering was done using Energy-dispersive spectroscopy

2.4 Mechanical test

A Macro-hardness Brinell tester (Germany-produced) was used to measure the samples' hardness. It was calibrated with a diameter 2.5 mm ball with a (31.25) kg/mm2 applied force and an implantation time of 10 seconds under applied weight conditions. For every sample, three measurements were taken, and the behavior of the alloys was used to analyze by average value.

The science and technology of two surfaces that interact when topics and practices move is known as tribology. Among the main causes of material wastage or decrease in mechanical performance is wear, therefore, reducing it might eventually result in considerable savings. Wear and dissipated energy is most often the result of friction [15]. Using the pin-on-disc device type (PIN ON DISK TRIBOMETER model MT/60/H), a specific wet wear rate was determined. Table (3) provides an illustration of how SBF solution performs the test.

Table (3): Chemical Composition of the SBF Solutions [17].

Chemical Formula	Quantity (g)
NaCl	6.547
Na HCO_3	2.268
KCl	0.373
$MgCl_2.6H_2O$-	0.305
$CaCl_2$.$2H_2O$	0.368
$Na_2HPO_4.2H_2O$	0.178
Na_2SO_4	0.071
$(CH_2OH)_3CNH_2$	6.057

The weight of the substrate was measured and considered as the initial weight (w_o). It was inserted in the holder, making sure the end surface of the specimen was parallel to the disc surface. The holder was adjusted to get the desirable wear track radius of 6mm. The loads were (10N, 15N, and 20N). The specimen is weighed with a delicate balance (0.0001) before the test. Following the allotted time of 5, 10, 15, 20, 25, 30, 35, and 40 minutes, at 350 rpm of spin. Until 40 minutes have passed, the process is repeated. The rate of wear was ascertained as in[16]:

$$\text{Specific wear rate} = \frac{\Delta W}{S}\left(\frac{g}{cm}\right) \quad \text{.....eq.(1)}$$

Where:

ΔW = Weight lost (g)

S = Sliding distance (260m)

S = Sliding Velocity (m⁄sec) * time(sec)...eq.(2)

$$\text{Sliding Velocity} = \frac{\pi DN}{30*1000}$$

Where: D = wear track diameter of 10 mm was used.

N = Speed of rotation disk (350rpm)

3. Results and Discussion

3.1. X-ray diffraction (XRD) of the Powders and Specimens

The phases were recognized by comparing them with standard reference patterns JCPDS card numbers. Phase identification of the Ti-24Nb-4Zr-8Sn alloy substrate prior to MWCNT reinforcement is shown in Figure 2(a), where beta (β) is the only primary phase that appears. Based on the diffraction pattern of β, this phase can be associated with the crystalline planes in JCPDS card

numbers No. 44–1288. Figures 2(b to e) show the primary phases of beta (β) as shown in the crystalline planes in JCPDS card numbers No. 44–1288. The XRD patterns also confirm that no additional contaminations were introduced in the MWCNTs/Ti composites synthesized by the powder metallurgy process.

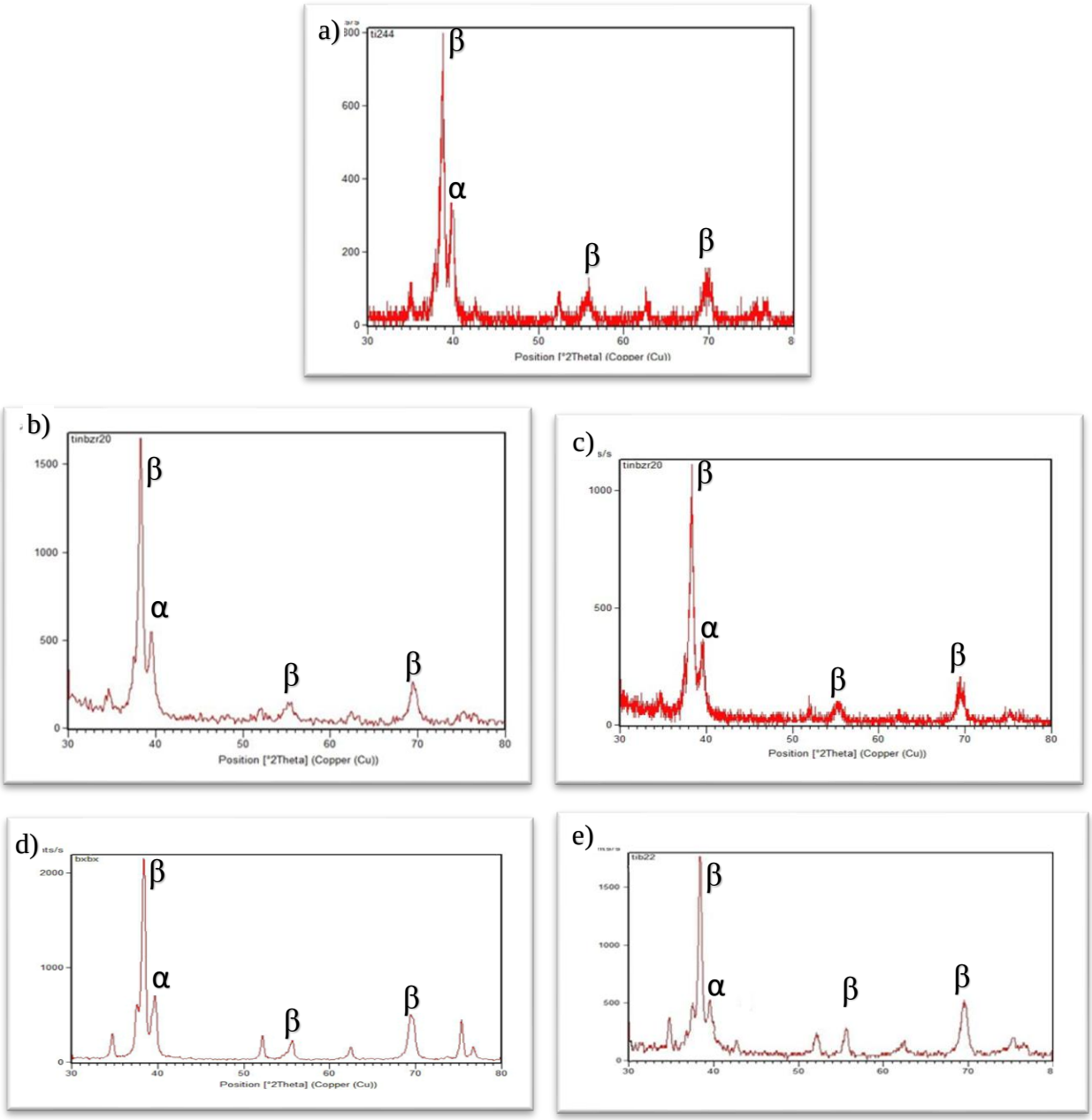

Figure (2): XRD for alloy a)M, b)A1, c) A2, d)A3 and e)A4

3.2. Grain Size Measurement

Figures (3) to (7) show the analysis of grain size for the prepared specimens. The results indicate that the average grain size of the base alloy Ti2448 sample was (48.91µm); by additional reinforcements, the grain size was reduced in different magnitudes, The ceramic particles are homogeneous distribution in the Ti matrix wanting any noticing of the reaction interface for Ti alloy. As a result, the grain size decreases as the content of ceramic particles is increased. The hardness of the ceramic particle has impeded grain growth in the sintering step, leading to a reduction in grain size and thus an improvement in the hardness of the consolidated samples. The reduction in the grain size maximizes the number of grain boundaries, causing improvement in the mechanical properties.

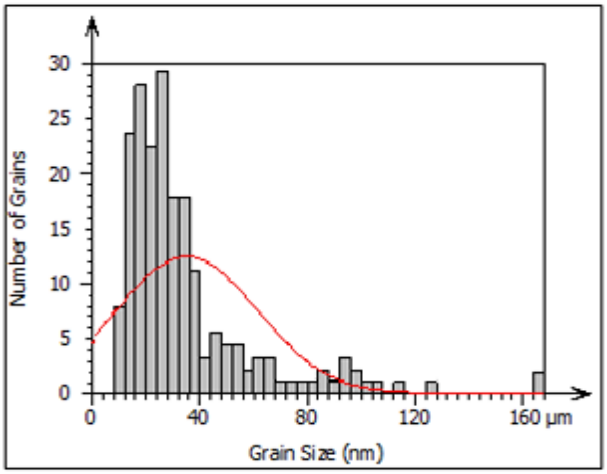

Parameters	Unit	Mean
Equivalent diameter	µm	48.91

Figure(3): Analysis of grain size for (M) sample

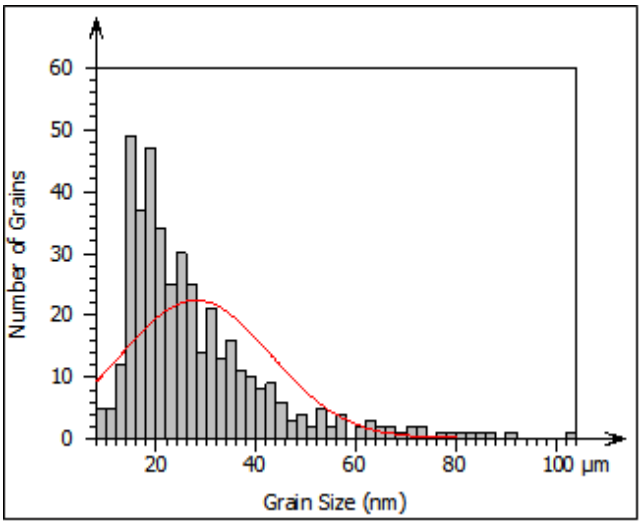

Parameters	Unit	Mean
Equivalent diameter	µm	27.95

Figure(4): Analysis of grain size for A1 sample

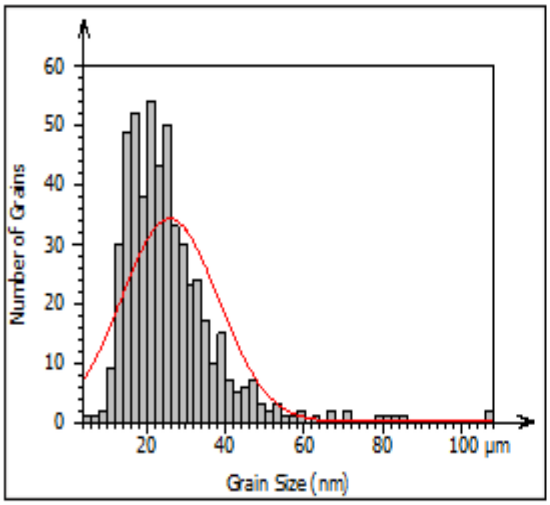

Parameters	Unit	Mean
Equivalent diameter	µm	27.23

Figure(5): Analysis of grain size for A2 sample

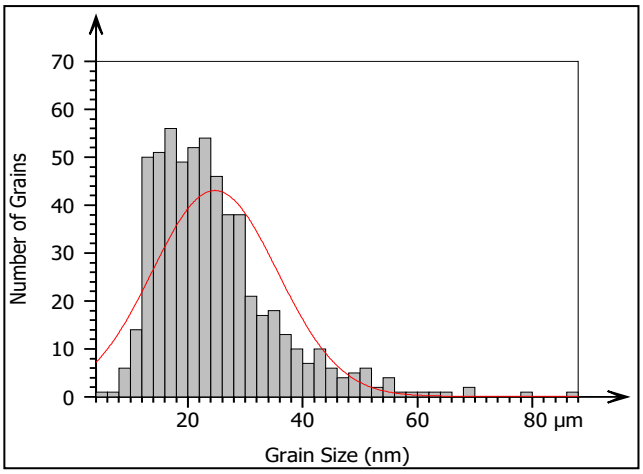

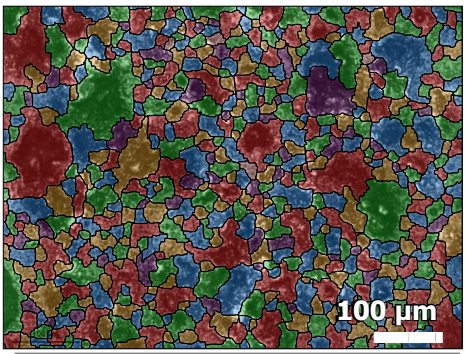

Parameters	Unit	Mean
Equivalent diameter	µm	25.83

Figure(6): Analysis of grain size for A3 sample

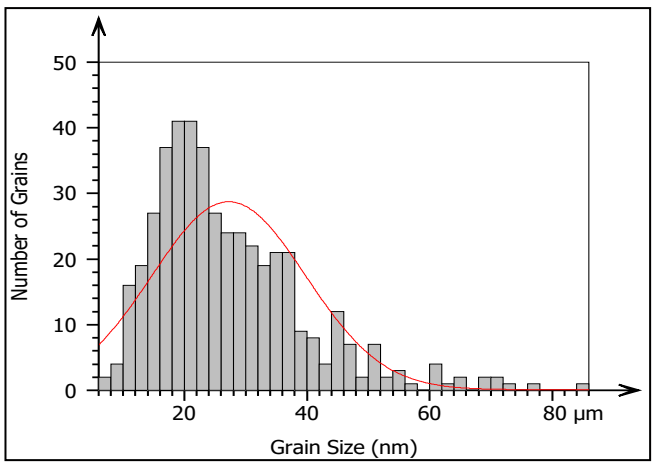

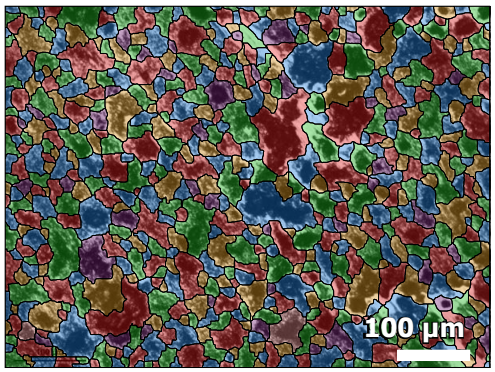

Parameters	Unit	Mean
Equivalent diameter	µm	23.70

Figure(7): Analysis of grain size for A4 sample

3.2 Light Optical Microscope (LOM)

Metallography gives an idea about material microstructure and its relationship to the characteristics of material because the size, shape, and distribution of the particles have significant effects on the behavior of a material[19]. The microstructure for alloys showed the grain boundaries, pores in different sizes, and the present phases. The microstructure reveals that all the specimen's alloys consist mainly of β phase as shown in Figure (8), the presence of the Nb element leads to showing dark region (β-phase) because of the effect of Nb as the Beta stabilizer element.as shown in figures(8):

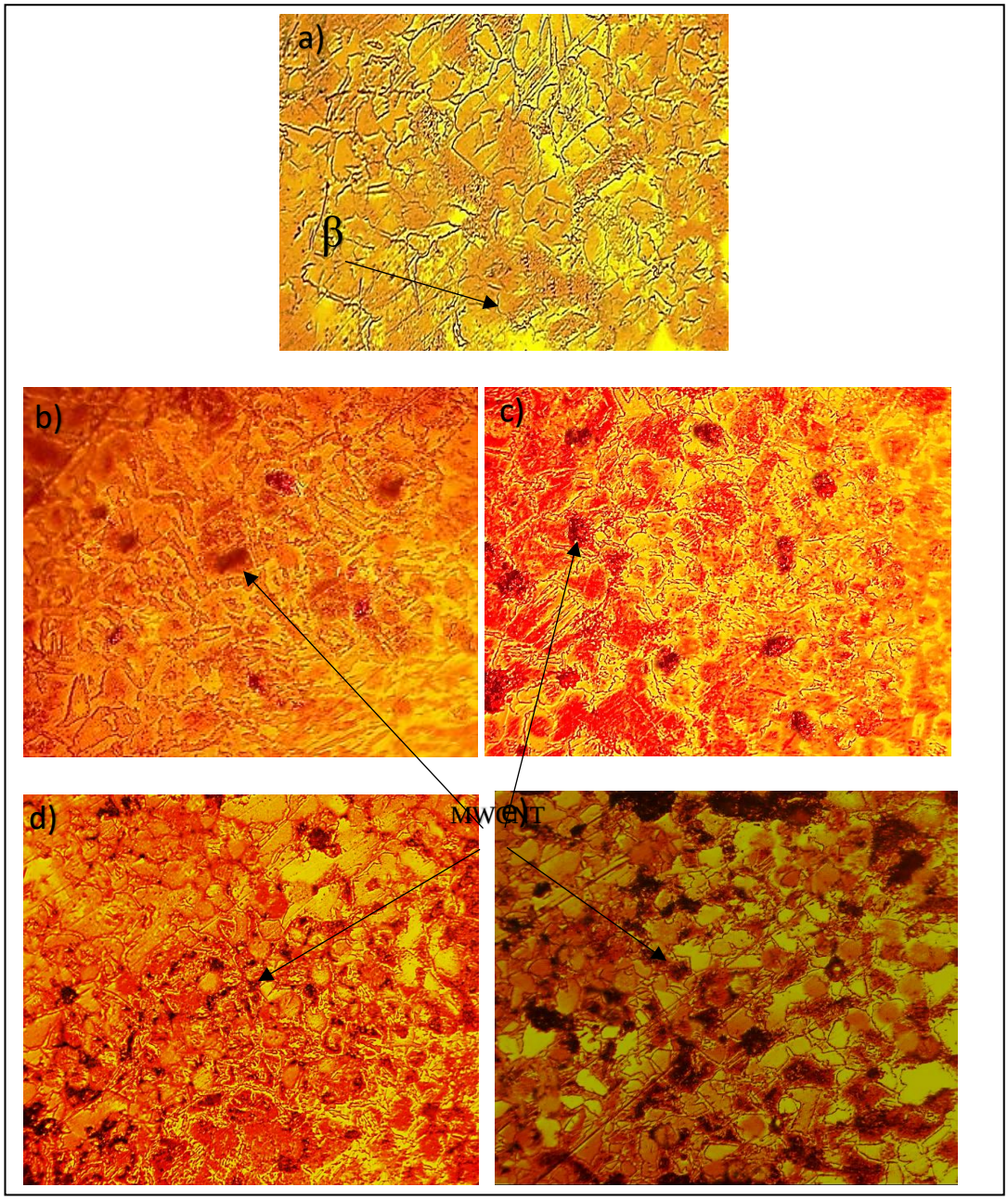

Figure (8): Optical Micrographs of a) M, b) A1, c) A2, d) A3, and e) A4 alloy with magnification(80X).

3.3 Scanning Electron Microscopy (SEM)

In SEM, the incident electrons transfer sufficient energy for electrons (secondary electrons) to be emitted from the sample. The intensity of the secondary electrons primarily depends on the topography of the surface. By scanning the electron beam across the samples and determining the current generated from secondary electrons, images of the surface are obtained figure (9) Thus, in contrast to the methods described previously, which provide surface chemical information SEM generally gives images reflecting surface topography.

The microstructure of the specimen's surfaces was studied by using an SEM test. Figure (9. a) shows the SEM of Ti-24Nb-4Zr-8Sn alloy (M) base alloy without addition. SEM are very sensitive to chemical composition as a result, the microstructure of sintered specimens showed a multiphase structure in which the two phases, mainly β and secondary α thus confirming the XRD results.

The SEM results of the microstructure specimen Figure (9. b,c,d,e) show that for surface morphology of the Ti-24Nb-4Zr-8Sn alloy reinforced by the different percentages of multi-wall carbon nanotube, the effect of adding MWCNT in the microstructure of the base alloy is clear, as the refining of the grain is due to the effect of MWCNT addition in impeding the growth rate of the grain as a result of their regular distribution on the base alloy[20,21].

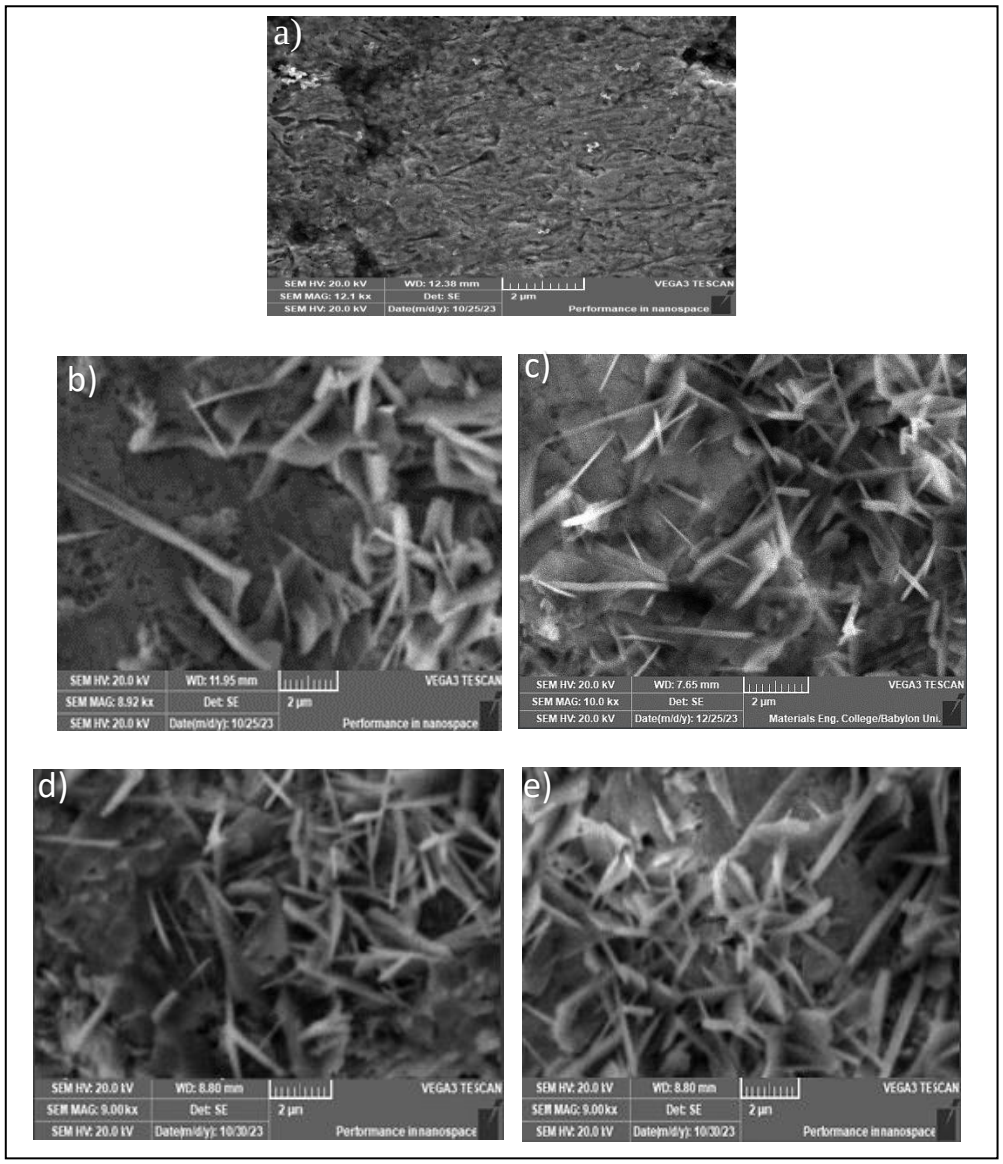

Figure (9): Micrographs of SEM specimen a) M, b) A1, c) A2, d) A3, and e) A4

3.4. Energy Dispersive X-ray (EDX) Spectroscopy

The chemical composition that emerges from variations in contrast topography on an SEM picture can be recognized using EDS. Statistical error restricts the precision that may be measured from samples. On a variety of polished specimens, EDS was scanned. Since the values obtained from the EDS study only cover the area where the electron made contact with the surface.as shown in figure (10-14).

Element	Weight %
Ti	49.9
Zr	2.0
Nb	38.6
Sn	9.5

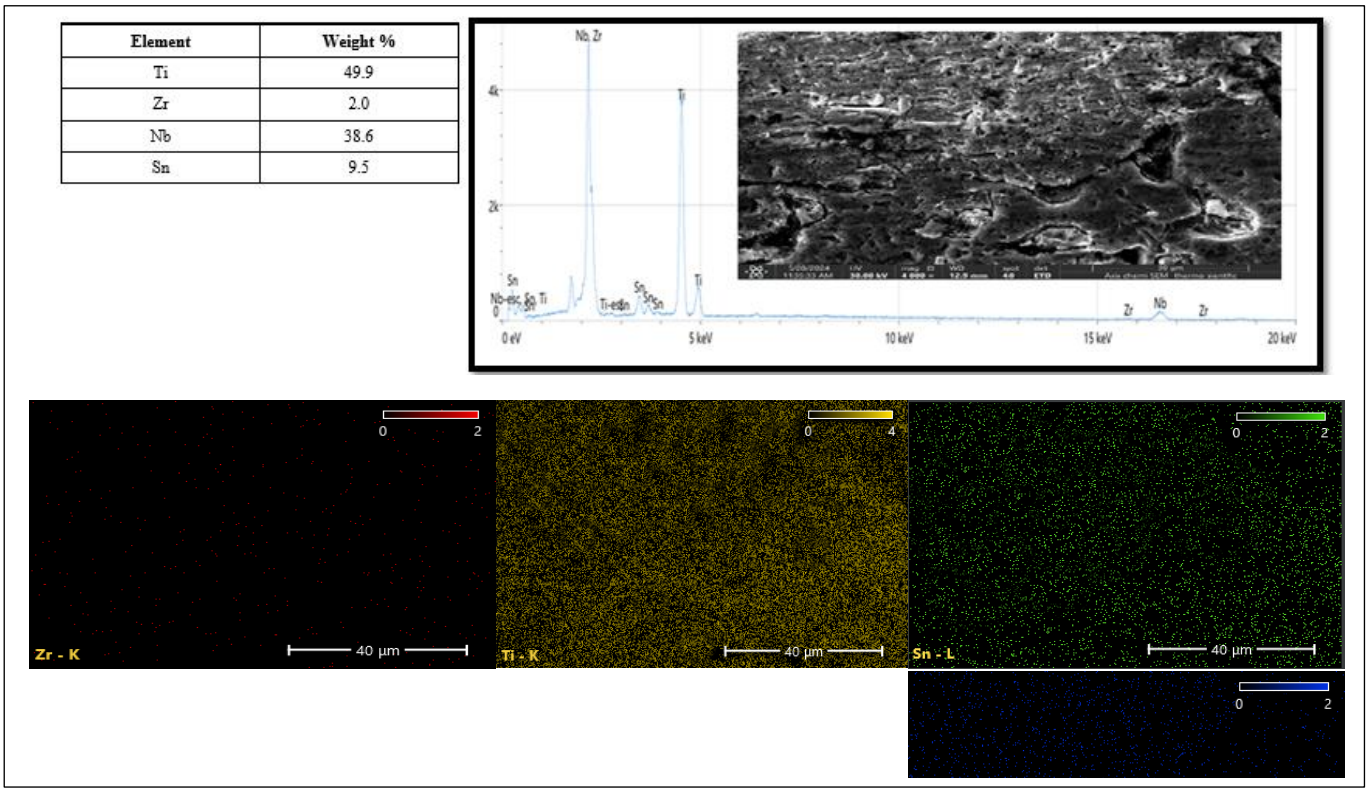

Figure(10):EDS for M alloy

Element	Weight %
C	9.6
Ti	68.3
Zr	2.0
Nb	13.4
Sn	6.6

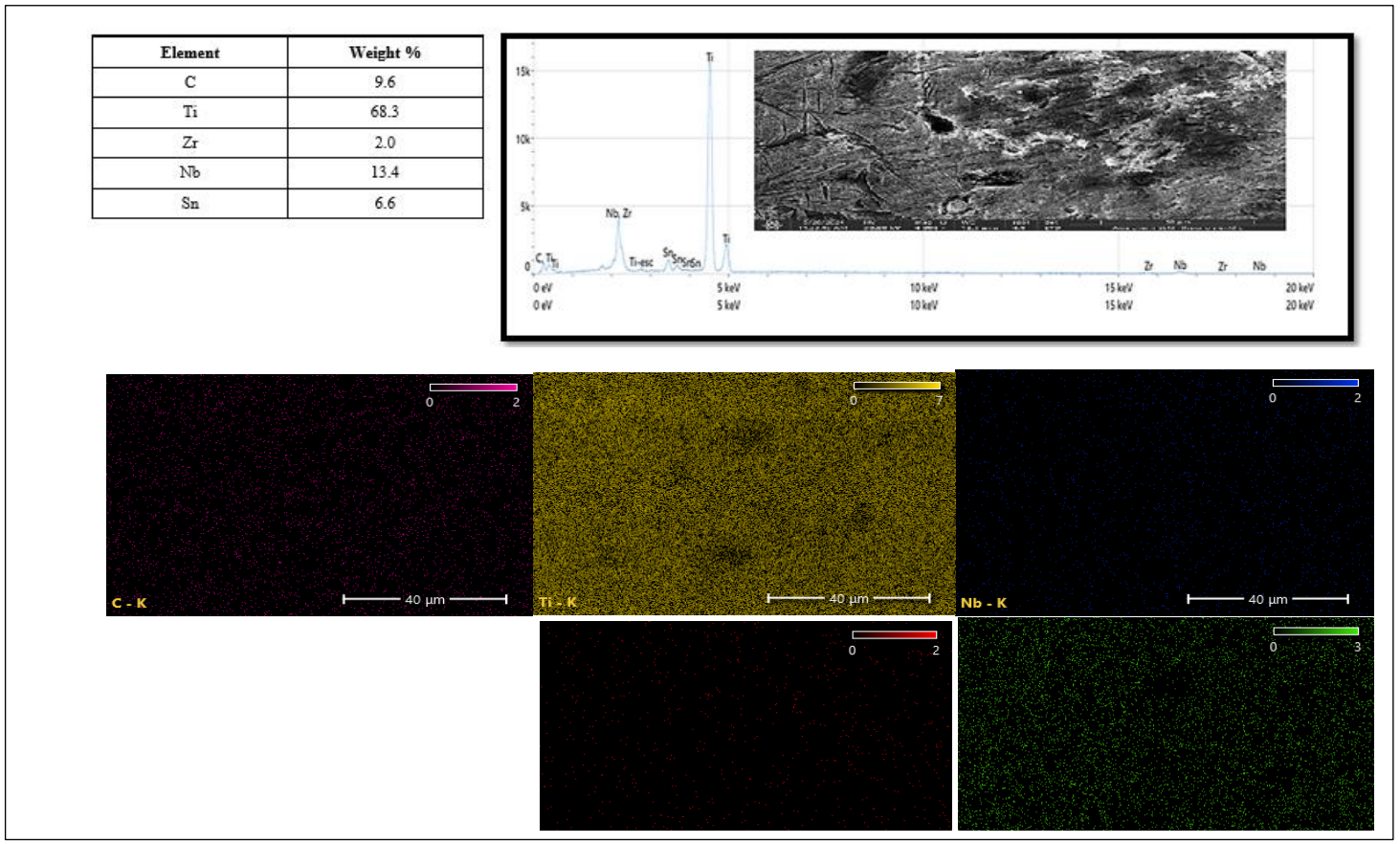

Figure(11):EDS for A1 alloy

Element	Weight %
C	11.5
Ti	47.1
Zr	2.3
Nb	32.5
Sn	6.7

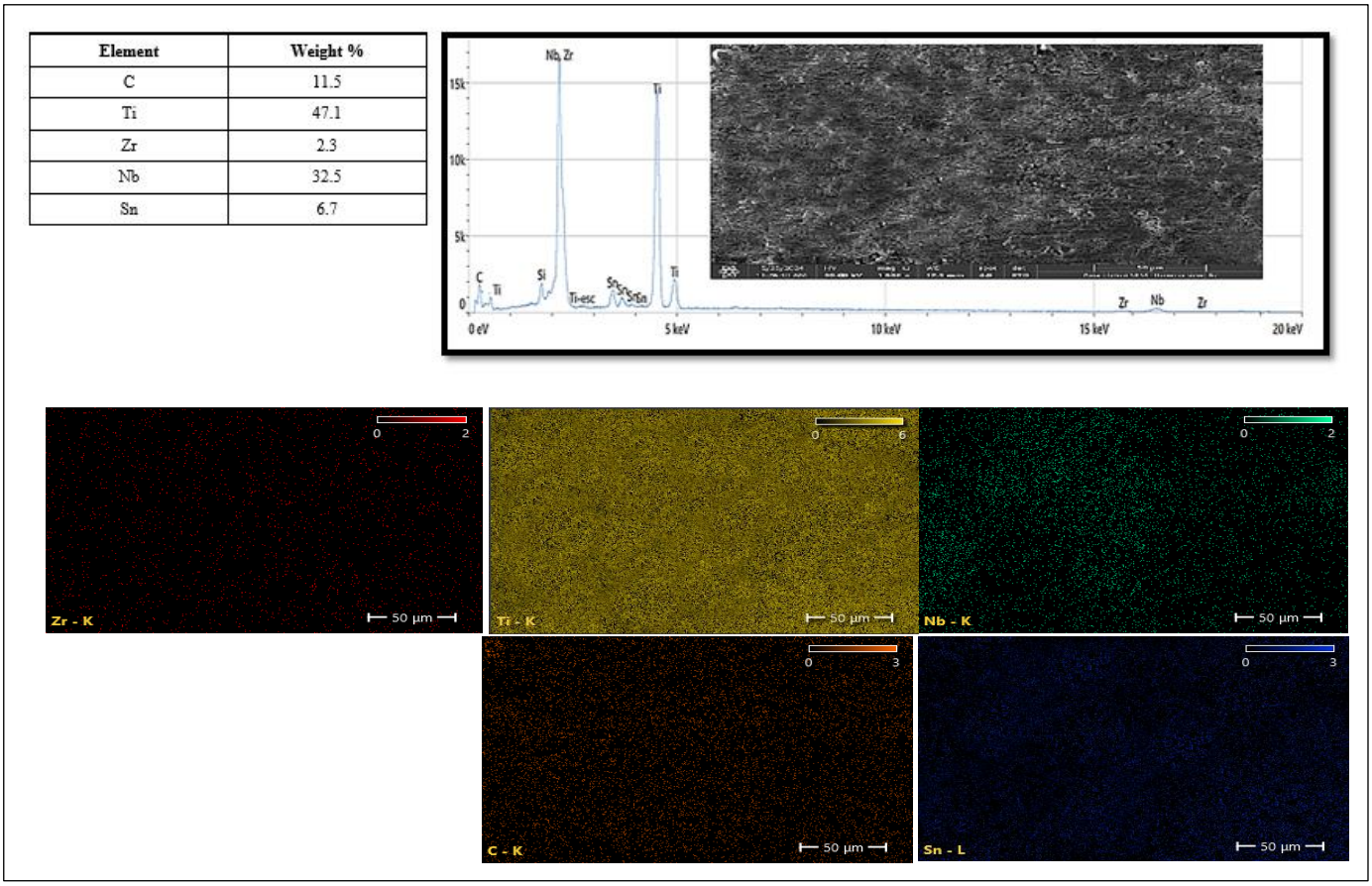

Figure(12):EDS for A2 alloy

Element	Weight %
C	15.7
Ti	53.7
Zr	2.1
Nb	25.1
Sn	3.5

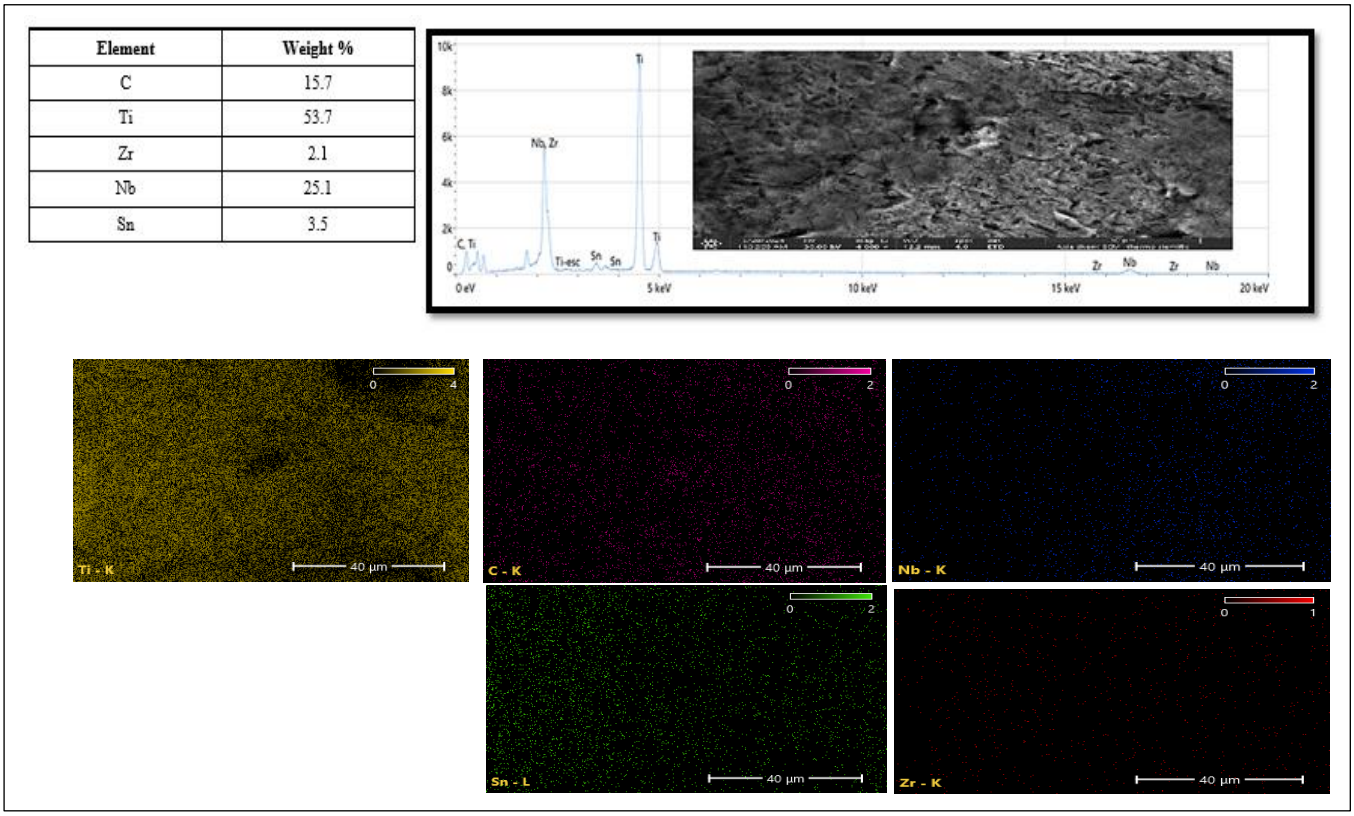

Figure(13):EDS for A3 alloy

Element	Weight %
C	16.2
Ti	58.7
Zr	3.2
Nb	16.7
Sn	5.4

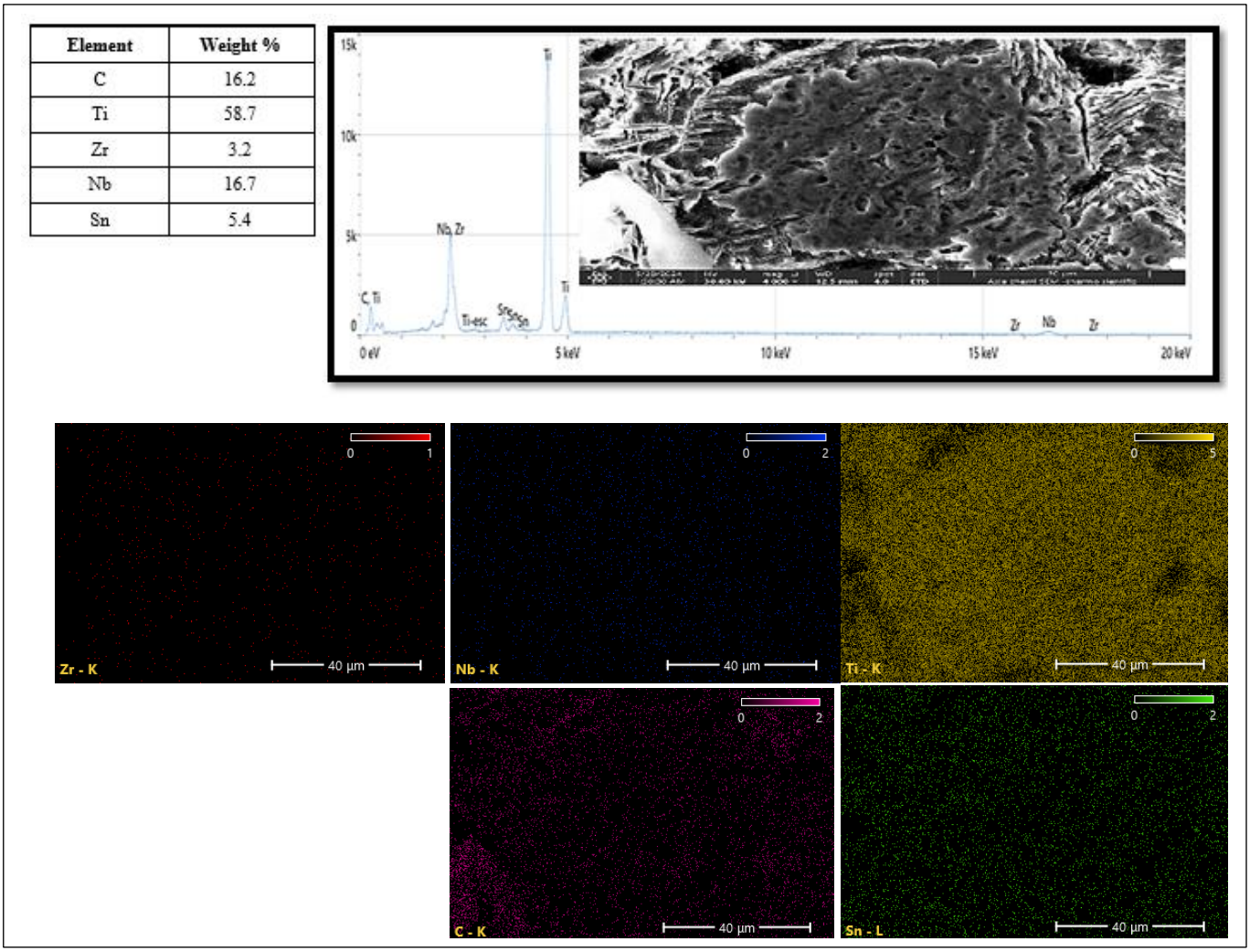

Hardness increases for developing specimens as the percentage of MWCNT increases. The hardness values in relative to the amount of MWCNT reinforcing are shown in (Figure 15). In actuality, reinforcements prevent dislocation motion during plastic deformation appropriate for increasing hardness[22].

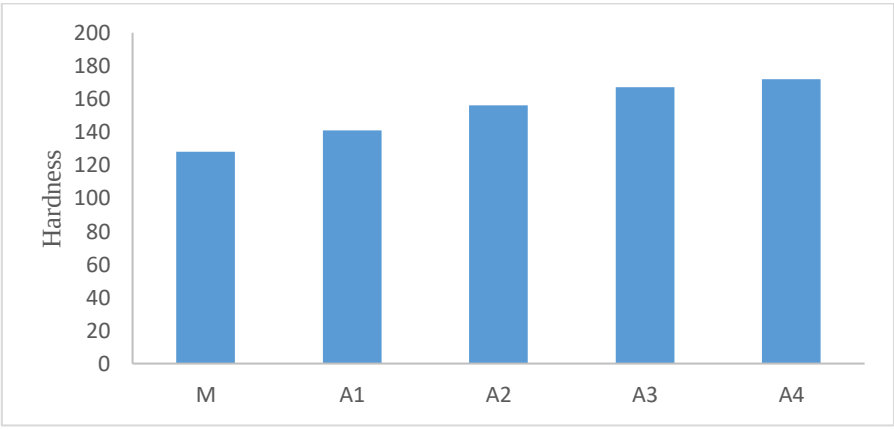

Figure (15): Effect of MWCNT content on hardness for Ti-24Nb-4Zr-8Sn alloy.

3.6 Wear test:

One of the most crucial mechanical characteristics of an implant is its resistance to wear, as wear failure is one of the main causes of implant failure. The wear mass loss of test specimens under 10N, 15N, and 20N loads and numerous times (5, 10, 15, 20, 25, 30, 35, and 40) min was utilized to calculate the wear rates generated by the pin-on-disc sliding wear test.

The wear rate is the highest value at which the applied load is 20 N. This is due to the fact that the weight loss rises when a high load is applied because the friction on the surface increases and the removal of the material is greater when the applied load increases because contact pressure and temperature between the sample and the steel pin increase this agree with[23, 24]. Generally, it was found that as loading time increased, the wear rate reduced. Superior wear resistance is provided by the more stable oxides (Nb_2O_5 and ZrO_2) that form on Ti-2448 alloy as a result of dissolution in SBF solution environment.

While adding reinforcing particles to the alloy slows down the rate of wear because it prevents the material from deforming plastically in comparison to the base alloy, this is also because the MWCNT particles added to the base alloy restricted the movement of the matrix and the boundaries between the grains, also, the addition of MWCNT has resulted in increasing hardness of the alloy and this would reduce wear rate as shown in the Figures(16-18) [25-29].

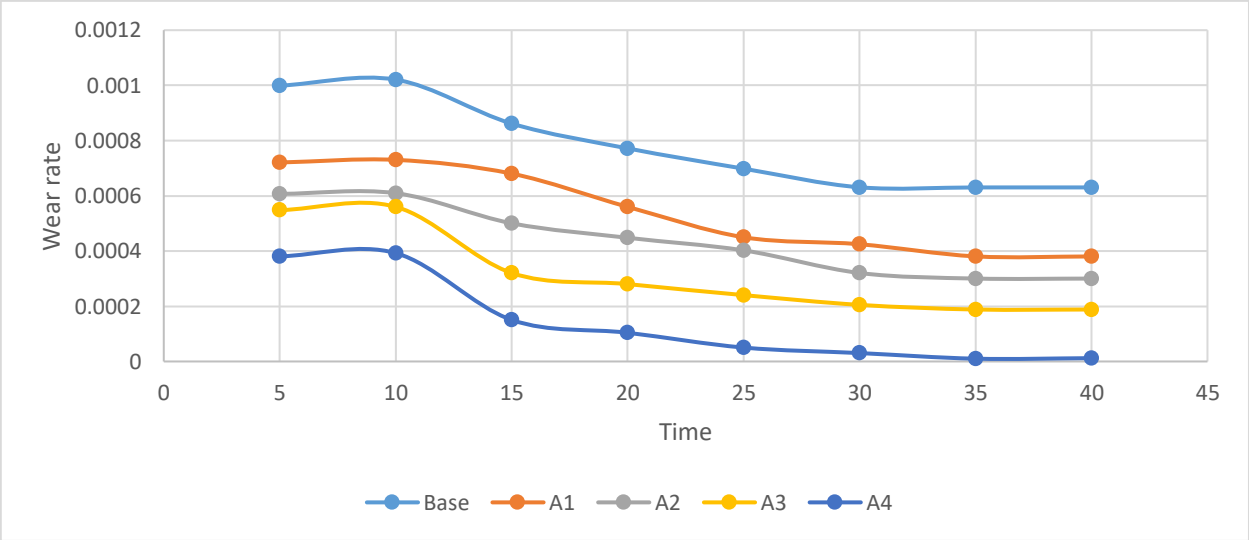

Figure (16): Correlation between test time and wear rate for Ti2448 alloy reinforced with varying MWCNT percentages under 10N load

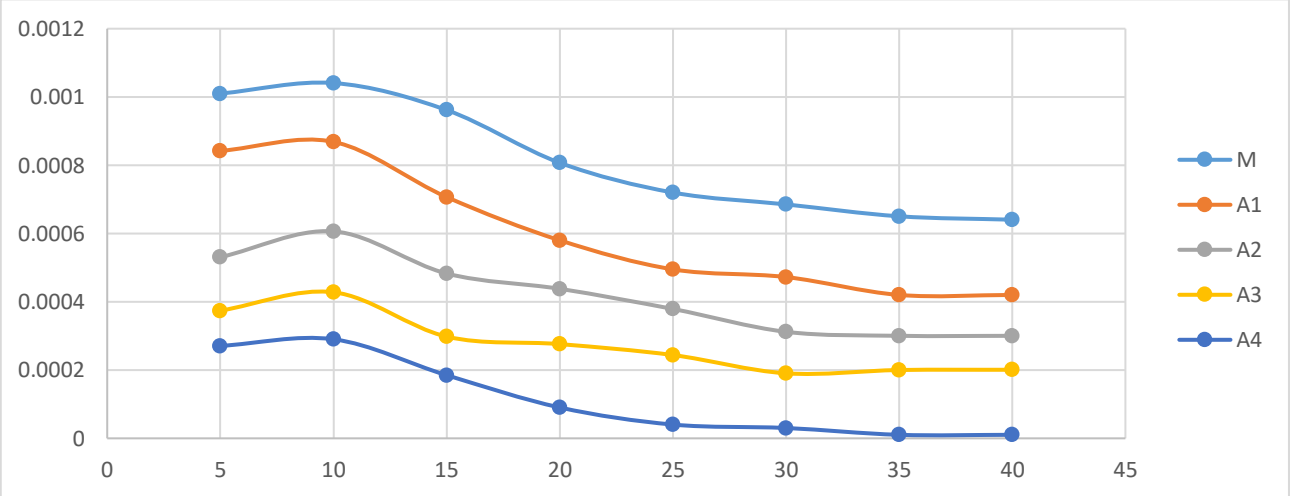

Figure (17): Correlation between test time and wear rate for Ti2448 alloy reinforced with varying MWCNT percentages under 15N load

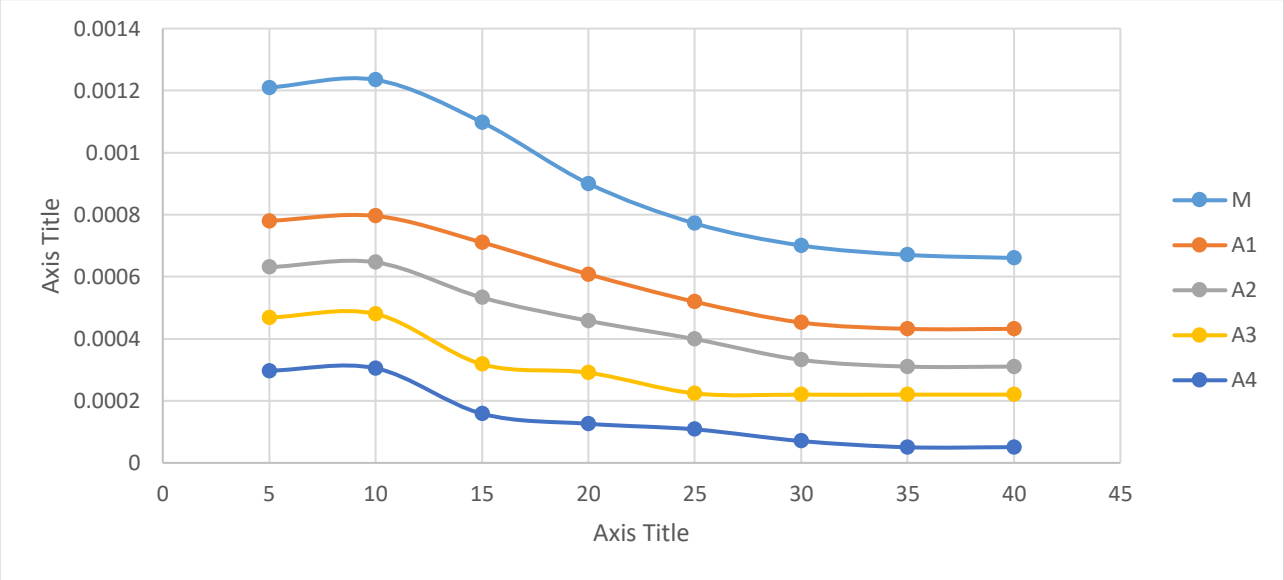

Figure (18): Correlation between test time and wear rate for Ti2448 alloy reinforced with varying MWCNT percentages under 20N load

References

[1] R.M. Pilliar, Overview of surface variability of metallic endosseous dental implants: textured and porous surface-structured designs, Implant Dent. 7 (1998) 305–314.

[2] M. Bahraminasab, B.B. Sahari, K.L. Edwards, F. Farahmand, M. Arumugam, T.S. Hong, Aseptic loosening of femoral components–a review of current and future trends in materials used, Mater. Des. 42 (2012) 459–470.

[3] M. Bahraminasab, M.R. Hassan, B.B. Sahari, Metallic biomaterials of knee and hip - a review, Trends Biomater. Artif. Organs 24 (2010) 69–82.

[4] S. Nag, S. Samuel, A. Puthucode, R. Banerjee, Characterization of novel borides in Ti–Nb–Zr–Ta+2B metal-matrix composites, Mater. Charact. 60 (2009) 106–113.

[5] J. Chevalier, L. Gremillard, Ceramics for medical applications: a picture for the next 20 years, J. Eur. Ceram. Soc. 29 (2009) 1245–1255.

[6] Vladimir A. Popov, Evgenij V. Shelekhov, Ekaterina V. Vershinina. Influence of reinforcing non-agglomerated nanodiamond particles on metal matrix nanocomposite structure stability in the course of heating. Eur J Inorg Chem 2016; 10:2122-2124.

[7] Hanada K, Yamamato K, Taguchi T, Osawa E, Inakuma M, Livramento V, et al. Further studies on copper nanocomposite with dispersed single-digit nanodiamond particles. Diamond Relat Mater 2007; 16(12): 2054–2057.

[8] Feng X, Sui JH, Feng Y, Cai W, Preparation and elevated temperature compressive properties of multi-walled carbon nanotube reinforced Ti composites. Mater Sci Eng A 2010; 527:1586-1589.

[9] Balandin A A, Ghosh S, Bao W, et al. Superior thermal conductivity of single-layer graphene [J]. Nano letters 2008; 8(3):902-907.

[10] Hao, Y. L., et al. "Super-elastic titanium alloy with unstable plastic deformation." Applied Physics Letters 87.9 (2005).

[11] L.C. Zhang, D. Klemm, J. Eckert, Y.L. Hao, T.B. Sercombe, Manufacture by selective laser melting and mechanical behavior of a biomedical Ti–24Nb–4Zr–8Sn alloy, Scripta Materialia 65(1) (2011) 21-24.

[12] Kafkas, Fırat, and Thomas Ebel. "Metallurgical and mechanical properties of Ti–24Nb–4Zr–8Sn alloy fabricated by metal injection molding." Journal of Alloys and Compounds 617 (2014): 359-366.

[13] M. P. Groover, Fundamentals of modern manufacturing: materials, processes, and systems. John Wiley & Sons, 2020.

[14] Iijimaa, D.T. Yoneyamab, H. Doib, H. Hamanakab, and N. Kurosakia " Wear properties of Ti and Ti–6Al–7Nb castings for dental prostheses " a Department of Oral Diagnosis and General Dentistry, Graduate School, Tokyo Medical and Dental University, vol. 45, no.1-5, pp.113-8549, 2003.

[15] Tavsanoglu and Tolga. "Deposition and Characterization of Single and Multilayered Boron Carbide and Boron Carbonitride Thin Films by Different Sputtering Configurations" PhD Diss. University Technique d'Istanbul, 2009.
[16] K. Praveenkumar, and V. R. Kabadi "Realistic Approach to Pin–on–D–Disc Wear Testing Measurement" International Journal of Advanced Production and Industrial Engineering, vol.610, pp.47-53, 2017.
[17] Mahdi, Ola Saleh. "'Preparation and Characterization of Hydroxyapatite from Bovine Teeth." Advanced in Natural and Applied Sciences 11 (2017): 623-630.
[18] Wei, Liangxiao, et al. "Synergistic strengthening effect of titanium matrix composites reinforced by graphene oxide and carbon nanotubes." *Materials & Design* 197 (2021): 109261.
[19] Ogden, H.R. and F. Holden, Metallography of titanium alloys. 1958: Titanium Metallurgical Laboratory, Battelle Memorial Institute.
[20] Kondoh, Katsuyoshi, et al. "Characteristics of powder metallurgy pure titanium matrix composite reinforced with multi-wall carbon nanotubes." *Composites Science and Technology* 69.7-8 (2009): 1077-1081.
[21] Wang, Fu-Chi, et al. "Rapid and low-temperature spark plasma sintering synthesis of novel carbon nanotube reinforced titanium matrix composites." *Carbon* 95 (2015): 396-407.
[22] Prakash, K. Soorya, et al. "Mechanical, corrosion and wear characteristics of powder metallurgy processed Ti-6Al-4V/B4C metal matrix composites." Ain Shams Engineering Journal 9.4 (2018): 1489-1496.
[23] Sozhamannan, G. G., M. Mohamed Yusuf, G. Aravind, G. Kumaresan, K. Velmurugan, and V. S. K. Venkatachalapathy. "Effect of applied load on the wear performance of 6061 Al/nano Ticp/Gr hybrid composites." *Materials Today: Proceedings* 5, no. 2 (2018): 6489-6496.
[24] Arul, S., Effect of nickel reinforcement on microhardness and wear resistance of aluminum alloy Al7075. Materials Today: Proceedings, 2020. 24: p. 1042-1051.
[25] Bai Y, Hao YL, Li SJ, et al. Corrosion behavior of biomedical Ti-24Nb-4Zr-8Sn alloy in different simulated body solutions. Mat Sci Eng C. 2013;33:2159–2167.
[26] Yu SY, Scully JR. Corrosion and passivity of Ti-13% Nb-13% Zr in comparison to other biomedical implant alloys. Corrosion. 1997;53(12):965–976.
[27] Cai Z, Shafer T, Watanabe I, et al. Electrochemical characterization of cast titanium alloys. Biomaterials. 2003;24(2):213–218.
[28] Tamilselvi S, Murugaraj R, Rajendran N. Electrochemical impedance spectroscopic studies of titanium and its alloys in saline medium. Mater Corros. 2007;58(2):113–120.
[29] Wang BL, Zheng YF, Zhao LC. Electrochemical corrosion behavior of biomedical Ti-22Nb and Ti-22Nb-6Zr alloys in saline medium. Mater Corros. 2009;60(10):1–7.